SUPPORTING INFORMATION

Design of Dual Hybrid Network Natural Rubber-SiO_2 Elastomers with Tailored Mechanical and Self-Healing Properties

*Mohammad Abdul Sattar [a, b], Shyju Gangadharan [b] and Archita Patnaik [a]**

[a]*Colloid and Interface Chemistry Laboratory, Department of Chemistry, Indian Institute of Technology Madras, Chennai-600036, India.*

[b]*R & D Centre, MRF Limited, MRF Road, Tiruvottiyur, Chennai 600019, India.*

CONTENTS

1. ADDITIONAL EXPERIMENTAL DATA:

Compounding procedure:

The NR-SiO_2 composites after liquid-liquid mixing were prepared on a two-roll mill. During mixing, the nip gap was 1 mm and the roll speed ratio was 1:1.2 for front and back rotors respectively with a roll speed of 27.5 rpm. First, NR-SiO_2 master batch was passed through the roller three times at room temperature followed by TESPT addition. Finally, the other compounding ingredients were added as listed in Table 3. After mixing, final composites were subjected to compression molding at 140 °C under 42 bar for 30 min towards obtaining tensile testing pads.

Supramolecular interactions in NR -SiO_2 composites: To confirm the H-bond interaction and the formation of a supramolecular structure in the nanocomposites, FTIR spectra of neat NR and the composites were acquired. Figure S1 shows obvious vibrational modes of pure NR, SiO_2 and NR-SiO_2 composites. In the spectrum of pristine NR, the characteristic absorption peaks at 1740 cm^{-1}, 1711 cm^{-1}, 1630 cm^{-1}, and 1543 cm^{-1} correspond to amine, ester, carboxyl, amide I, and amide II stretching frequencies respectively. Amide I and II bands are specific to peptide bonds and are linked to the protein part of NR[1-2]. On the other hand, ester and carboxyl groups are mostly present on lipid molecules. The spectral region 1780-1500 cm^{-1} is used to probe the NR-SiO_2 interactions. Compared to the pure NR, it can be noted that the absorption bands at 1740 cm^{-1}(ν R_1-(C=O)-O-R_2) and 1711 cm^{-1} (ν R_1-(C=O)-OH) broadened and shifted to lower

wavenumbers 1737 cm^{-1} and 1696 cm^{-1} respectively indicating the formation of supramolecular network between silica surface silanol groups and the lipid groups of NR. Further, the intensity of the band at 1543cm^{-1} (β N-H + ν C-N of proteins) decreased and broadened indicating the participation of non-rubber components (proteins of NR). Thus, the self-assembly of NR and

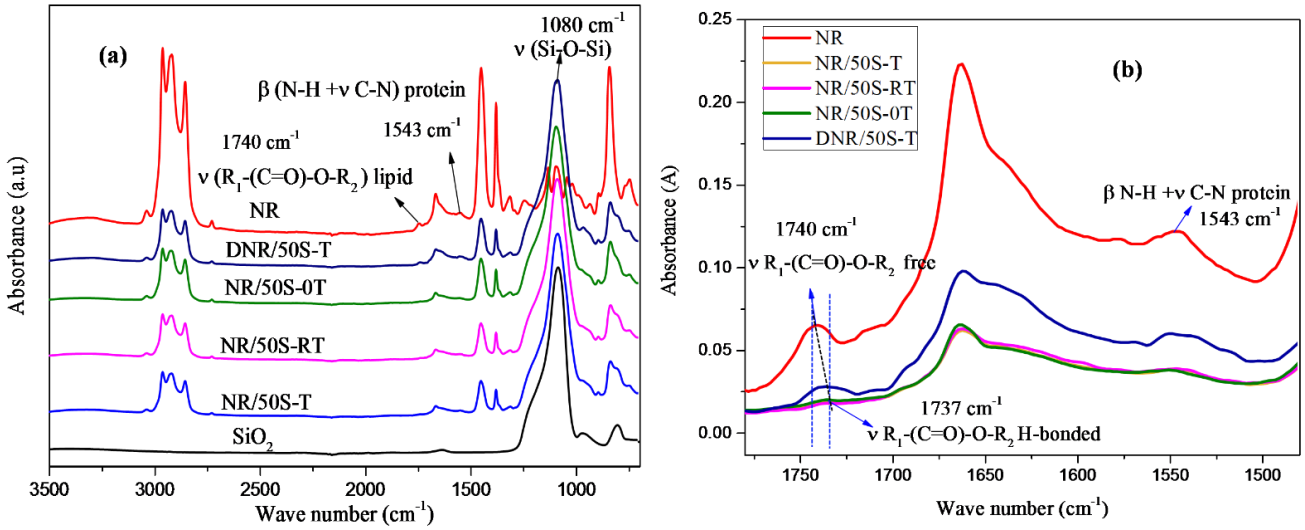

Figure S1: (a) FT-IR Spectra of pristine NR and NR-SiO_2 composites (b) FT-IR Spectra of neat NR and NR-SiO_2 composites depicting the H-bonding in the ester and amide regions of NR.

SiO_2 in the resultant composites was stabilized by the formation supramolecular networks supported by H-bonding interactions. Additionally, we observed that in liquid mixing the interaction is driven by the hydrophilic bioshell of NR, in contrast to dried conditions, where hydrophobic polymer dominates the interaction of NR with the SiO_2. Consequently, the spectral bands related to specific non-rubber components (Lipids and Proteins) of NR are less affected in DNR/50S-T prepared under dry conditions. The location of the peak absorbance near 1080 cm^{-1} was followed to determine the SiO_2-SiO_2 interactions in the composites, vide Figure S2, SI. The current changes in the Si-O-Si spectral region arose from the combination of physisorption and chemisorption of NR chains on to the filler surface. As shown in Figure S2 the stretching

frequency of Si-O-Si peak for pristine SiO_2 (1080 cm^{-1}) was shifted to higher wave number in the composite containing 25 phr SiO_2 loading, while it was shifted to lower wavenumber at high silica loading (75 phr). Such frequency shifts can be attributed to the restricted degree of silica dispersion in the NR matrix and clustering of filler particles.

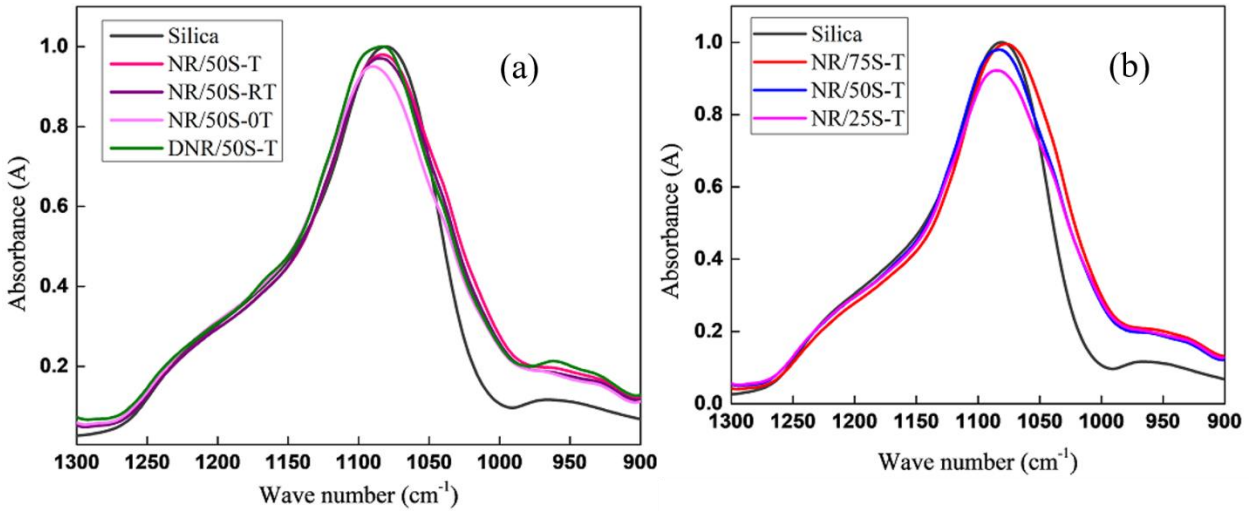

Figure S2: (a) and (b) FT-IR Spectra of pristine SiO_2 and NR-SiO_2 composites depicting the changes in asymmetric Si-O-Si stretching frequencies in silica region.

Interfacial Adhesion and Dispersion in NR-SiO_2 Composites: The polymer-filler interfacial interactions are critical for the properties of the final composites. The composite structures were characterized by TEM. Owing to large polarity difference between silica and NR the apparent silica aggregates comprising of primary silica clusters are observed in the NR-SiO_2 composites, as shown in Figure S3. For NR/50S-0T composite, the dispersion of silica is modestly improved in view of Mg^{2+} behaving as a salt bridge between NR and silica. Further, the dispersion of silica is poor in DNR/50S-T composite with large silica aggregates. Here, in dry compounding process, the reaction takes place in highly viscous rubber melt where TESPT molecules cannot competently graft onto silica, leading to a poor compatibility between NR and SiO_2. However, a relatively uniform dispersion throughout the NR matrix with fewer aggregates

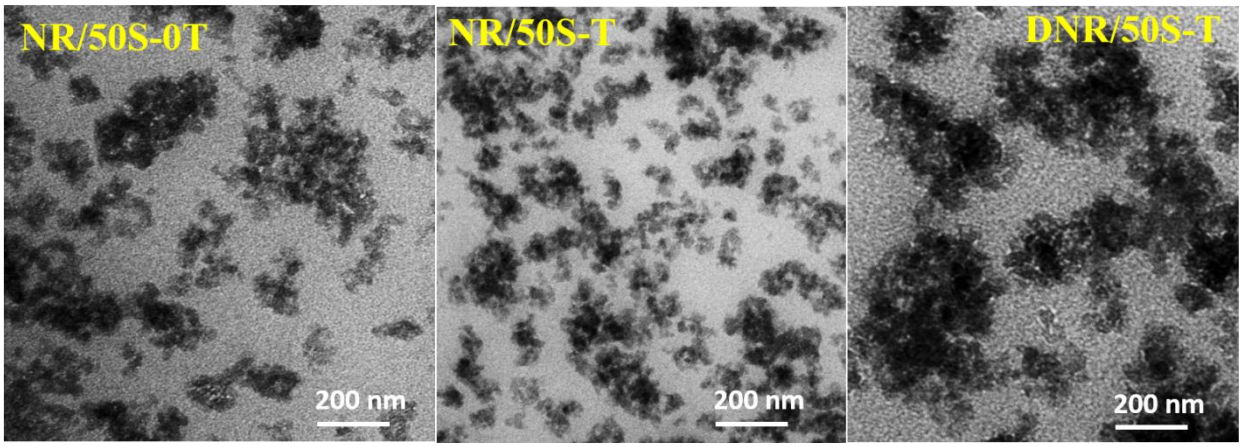

Figure S3: TEM pictures of NR-SiO_2 composites prepared via liquid -liquid mixing approach and dry mixing process respectively.

was noticed in NR/50S-T composite. It is obvious that the silanization extent of silica is promoted in NR/50S-T composite because of pre-dispersed silica achieved via Mg^{2+}. Concomitantly, the number of surface silanol groups is decreased, which alleviates the self-aggregation of silica. In addition, the interfacial interaction between silica and NR is improved due to covalent grafting of TESPT. Simultaneously, the tetrasulfide moiety of TESPT cross-links the NR chains during vulcanization and promotes the adhesion between NR and SiO_2.

Such interactions prevent the thermodynamically favorable reaggregation of silica in the final polymer composite.

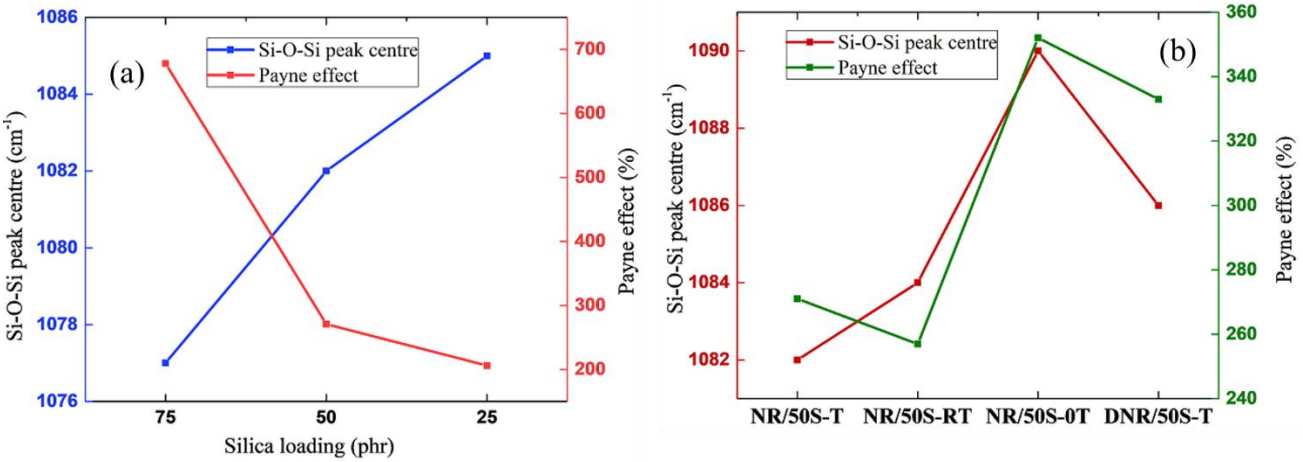

Figure S4: The correlation between the shift in asymmetric Si-O-Si peak center in silica region and the Payne effect of NR-SiO_2 composites (a) at various silica loading and (b) at similar filler loading but varied TESPT levels.

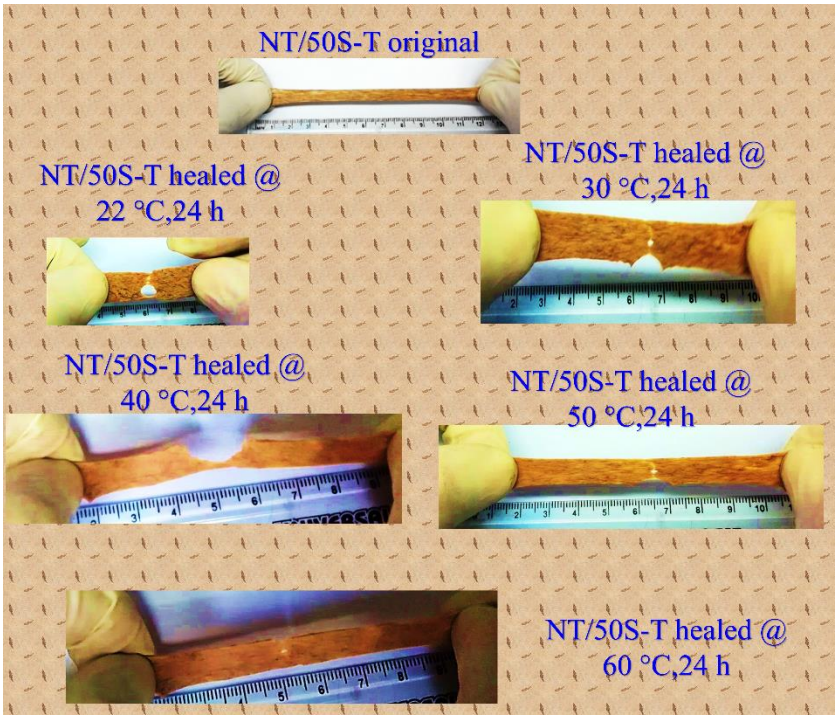

Figure S5: Photographs of NR/50S-T composite illustrating self-healing behavior after 24 h healing time at various temperatures.

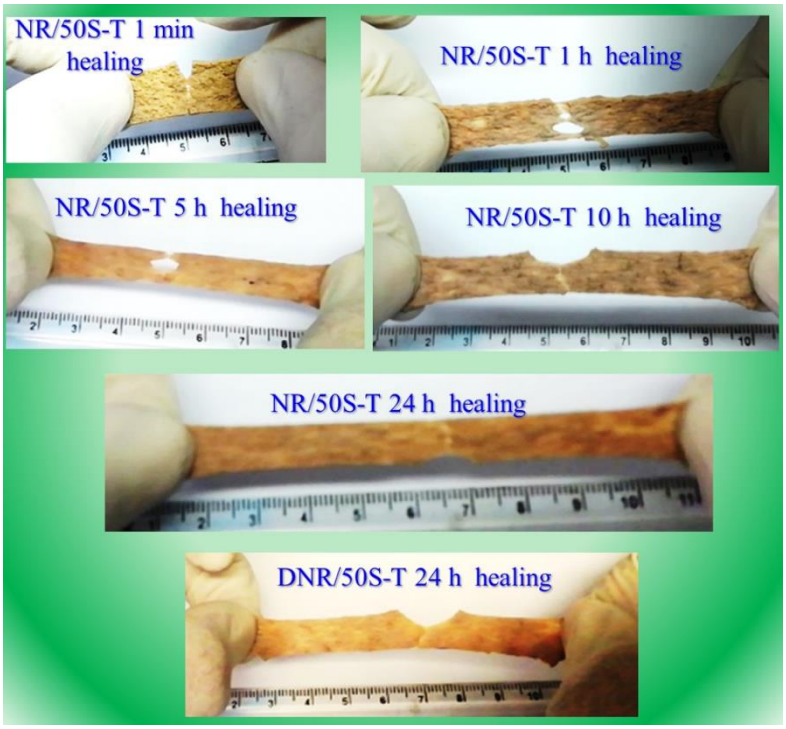

Figure S6: Photographs of NR/50S-T composite illustrating self-healing behavior at 50˚C after various healing times.

2. ADDITIONAL DATA

Table S1. Surface area and pore size analysis of Silica.

	Specific surface area (m^2/g)	Pore volume (cc/g)	Pore diameter Å	# OH /nm^2
silica	193	0.42	78.5	8.3

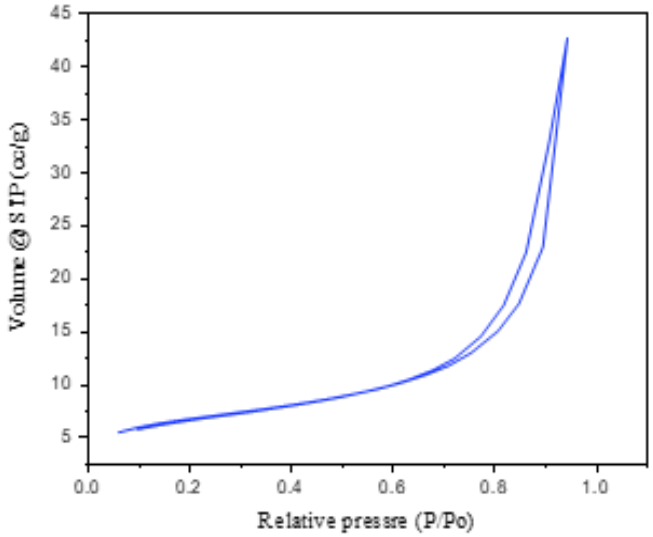

Figure S7: BET isotherm of silica

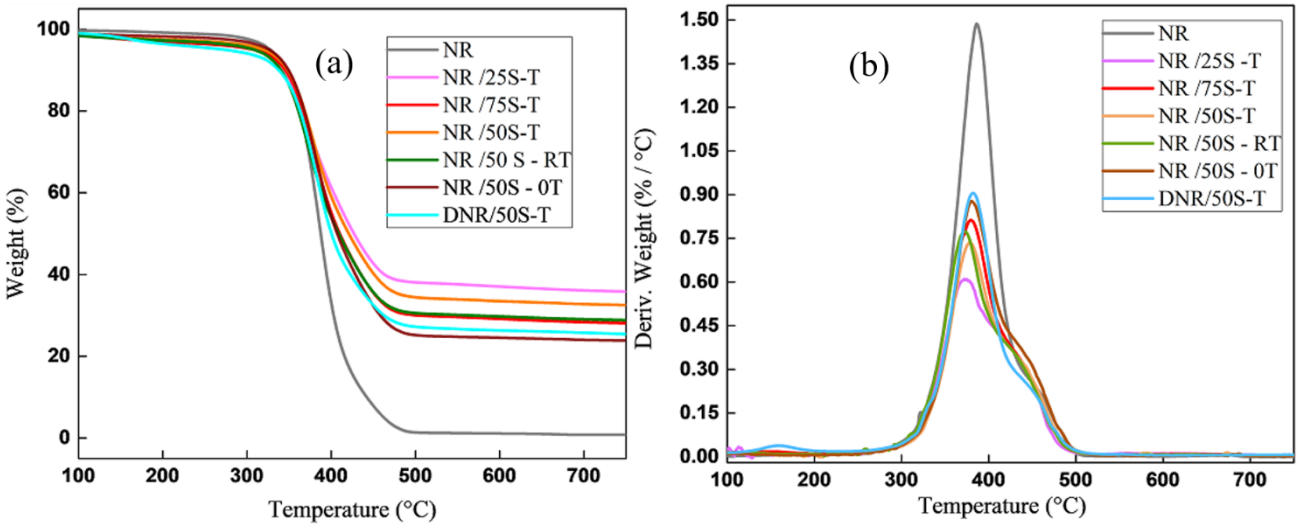

Figure S8: Thermal stability of pristine NR and NR-SiO_2 composites (a) Normal mode and(b) derivative mode

The TGA and DTG curves for the various samples are illustrates in Figure S8 (a, b). The extended thermal stability of the composites was ascribed to the stronger interactions between NR and silica arising from constrained NR chains with high physical intercalation , entanglement and interlock inside the mesoporous silica, in addition to the covalent cross-links via TESPT.Thermal decomposition occurred mainly in the range 300 to 500 °C for neat NR, whereas the thermal degradation behavior for all NR-SiO_2 composites occurs with a single major mass loss step similar to that of NR, along with a shoulder peak as found in DTG curves.

The swelling of NR-SiO_2 composites in aqueous medium was done at room temperature by immersing the circular sheets of the composites with 20 mm diameter and 1mm thickness. At specific time intervals, the sheets were removed and the surface was wiped off with a dry cloth and weighed again. Following this the samples were immersed again in water wherein the water uptake was estimated from the relative weight gain pf the sample according to the equation $W_u = \frac{M_t - M_0}{M_0} \times 100$ wher, M_0 and M_t are the sample weights before and after time t.

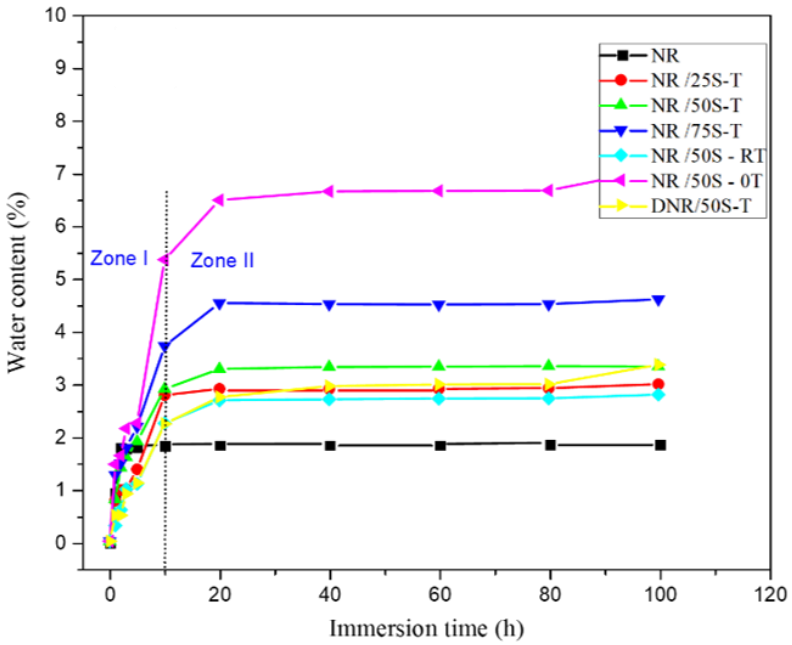

Figure S9: Water uptake measurements depicting the water transporting properties of the NR-SiO_2 composites.

Figure S9 shows the water absorption behaviour of the composites at specific time intervals where two zones were identified corresponding to i) fast absorption kinetic region (t < 10 h) and ii) plateu like zone associated with slow water uptake kinetics.[3-4] NR being hydrophobic in nature restricts the diffusion of water molecules. The presence of surface silanol groups on silica adsorbs water via H-bonding interactions and therefore aid water diffusion. From Figure S9 it is obvious that the water adsorption for all composites increased with increase in SiO_2 content until an equilibrium state was achieved. Further it is clear that NR/50S -0T with no TESPT has 7.1 % water uptake after 100 h which is 3.9 times higher than neat NR. However, the presence of TESPT makes the silica surface more hydrophobic and slows down the water diffusion rate. For example, the water uptake for NR/50S-RT after 100 h loading is 2.9 % only 1.6 times higher than NR. These results are in good agreement with BR content studies which indicates efficient grafting of TESPT on to the silica surface even at lower TESPT levels (2.5 phr).

References:

1. Rolere, S.; Liengprayoon, S.; Vaysse, L.; Sainte-Beuve, J.; Bonfils, F. Investigating natural rubber composition with Fourier Transform Infrared (FT-IR) spectroscopy: A rapid and non-destructive method to determine both protein and lipid contents simultaneously. *Polymer Testing* **2015,** *43*, 83-93.
2. Xu, T.; Jia, Z.; Wu, L.; Chen, Y.; Luo, Y.; Jia, D.; Peng, Z. Influence of acetone extract from natural rubber on the structure and interface interaction in NR/silica composites. *Applied Surface Science* **2017**, *423*, 43-52.
3. Yu, P.; He, H.; Luo, Y.; Jia, D.; Dufresne, A. Reinforcement of Natural Rubber: The Use of *in Situ* Regenerated Cellulose from Alkaline-Urea-Aqueous System. *Macromolecules* **2017**, *50* (18), 7211-7221.
4. Guo, B.; Tang, Z.; Zhang, L. Transport performance in novel elastomer nanocomposites: Mechanism, design and control. *Progress in Polymer Science* **2016**, *61*, 29-66.